Chapter 1

Experiment

1.1 Discharge Apparatus

The RPND apparatus used in the forthcoming experiments was similar in design to the coaxial geometry used by Vasilyak and others in their FIW studies [1]. It can be described as a cylindrical inner conductor, surrounded by a dielectric, covered by an outer conductor. In this case, the anode and the RPND served as the inner conductor. The dielectric was provided by a glass tube and an air gap. Finally, the outer conductor was a series electrically connected metal shells which served as the current return path. The geometry and its electrical equivalent are sketched in figure 1.1. Following from right to left, the inner conductor was composed of a vacuum window, a nipple, a double-sided flange tapped for an NPT connection, and the discharge tube containing the RPND. Unless otherwise noted, all vacuum components featured DN35 CF flanges with copper gaskets.

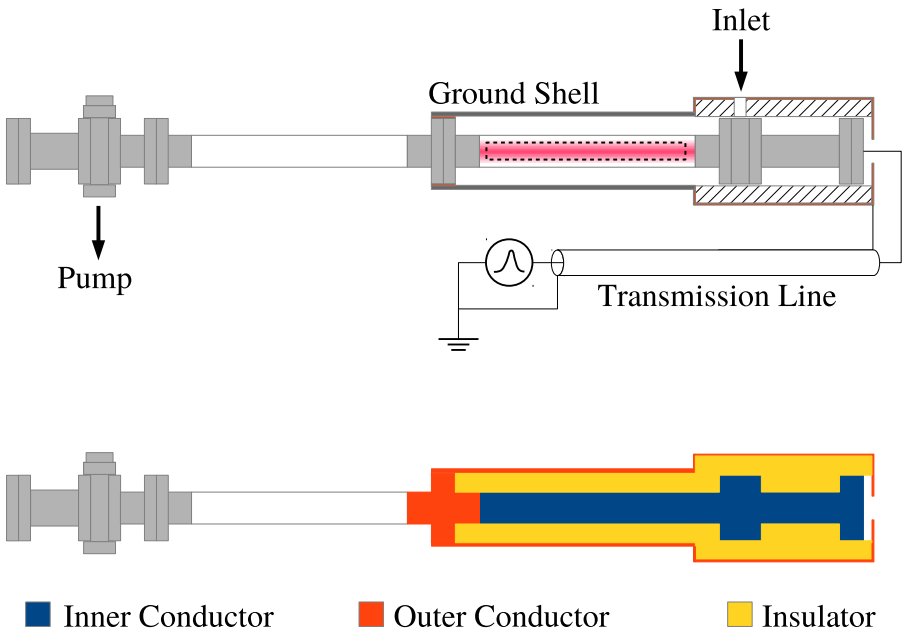

Figure 1.1: Two illustrations of the RPND apparatus. The upper version is an annotated sketch of the device, and the bottom version simplifies the geometry into its three electrical components.

The tube was composed of borosilicate glass with metal vacuum flanges on both ends. The flanges of the tube also acted as the electrodes for the generation of the RPND. The glass tube had an inner diameter of 3.3 cm, an outer diameter of 4.0 cm, and a length of 22.9 cm. The overall length of the tube including the flanges was 30 cm. In the figure shown here, the right electrode served as the anode, and the left electrode was the cathode.

The dielectric surrounding the inner conductor was composed of several components. The vacuum window, nipple, double-sided flange, and anode were separated from the outer conductor by an air gap and a polytetrafluoroethylene (PTFE)

tube, 20 cm in length with an inner diameter of about 7.5 cm, and an outer diameter of 10 cm. The RPND portion of the inner conductor was separated from the outer conductor by the glass tube and an air gap of about 2.54 cm.

The left side of the discharge tube, or cathode, connected to the outer conductor and served as part of the current return path. Directly attached to the cathode was an alumninum tube, held in place by an acetyl resin shaft collar and a copper shim. Radial optical access to the discharge was provided by two slots milled into the ground shell. The slots were positioned on opposite sides of the shell and were 3.8 by 25.4 cm in length. The tube itself was 30 cm in length.

The end of the aluminum tube nearest the anode was affixed to a copper sheet which was oriented perpendicular with respect to the tube's axis of rotation. The sheet was 10 cm square, and was attached to the tube with conductive copper tape. A 5 cm diameter hole was cut into the copper sheet to allow the discharge tube to pass through it. The sheet was secured to the edge of the PTFE tube by nylon screws. Surrounding the PTFE tube was a second shell, made of rolled copper sheet. This was electrically connected to the aluminum tube by a braided copper strap. The right end of the PTFE tube was covered by a second copper sheet, 10 cm square. Again, the sheet was secured to the PTFE tube by nylon screws and in electrical contact with the copper shell. In the center of the copper sheet was a HN bulkhead adapter for connection to the transmission line. The inner conductor of the bulkhead adapter was connected by a straight run of 5 cm of silicone-coated wire to the vacuum window flange. The outer conductor of the bulkhead adapter

provided the ground connection for the discharge apparatus.[1]

The voltage pulse was generated by a FID power supply, supplied by ANVS, Inc. (model PT510NM). The amplitude of each pulse was fixed at 6.4 kV with a repetition rate of 1.0 kHz. Each pulse had a fixed width of 25 ns, with a 10%-90% rise time of approximately 4 ns and was roughly Gaussian in shape.A SRS DG645 delay generator was used to trigger the power supply output for all experiments and provided a reference time base for all measurements.

Preliminary experiments revealed multiple reflections between the power supply and the anode. A 13.7 m transmission line, made of RG213 coaxial cable, was used to temporally separate the reflections so that the effects of the individual pulses could be studied. The calculated delay introduced by the transmission line was 69.2 ns. As the reflection would have to cross the length of the transmission line twice before it reached the anode again, the total separation time between the initial pulse and each subsequent reflection was 138.4 ns. This calculated delay was found to be a close match in the measured delay.

A simplified version of the gas flow system can be seen in figure 1.2. The gas supply was provided by a bottle of ultra-high purity helium. Following the regulator, the helium passed through a digital flow controller which was set at 25.0 sccm for all experiments. The helium then entered a gas distribution manifold, followed by a shutoff valve, a short run of 1/4" stainless steel tubing, another shutoff valve, about 2 m of 1/4" polyethylene tubing, and then the discharge tube

[1] Measurements confirmed that the entirety of the outer conductor had a low DC impedance to ground. However, it is likely that at frequencies relevant to the RPND, the impedance is not negligible. As a result, the outer conductor likely floats to a finite voltage during operation.

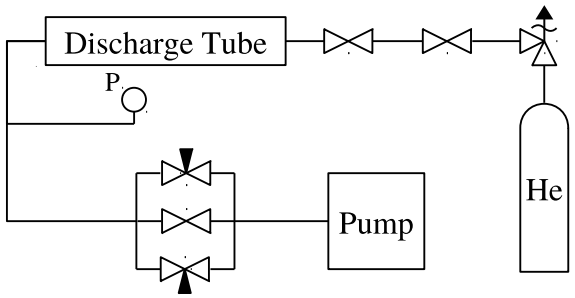

Figure 1.2: Simplified diagram of the gas flow path and pumping system.

via the double-sided flange.

The gas exited the discharge tube via an identical tube, on the side opposite the inlet, see figure 1.1. This second tube was intended to electrically isolate the discharge portion of the apparatus so that only a single conductive path to ground existed. The pressure was monitored downstream of the second tube with two capacitance manometers (one with a full scale range of 10 Torr, the other with a range of 100). Following that, the second tube was connected to an oil-seal roughing pump via three independent paths. The primary pump path had the highest gas conductance and was controlled by a bellows valve. However, this path was typically closed in favor of two needle valve bypasses. The needle valves were used to control the pumping speed and obtain the desired operating pressure. Immediately upstream of the roughing pump was a zeolite trap in order to limit oil backstreaming.

The base pressure of the system was measured to be approximately 15 mTorr. The leak rate was measured several times by evacuating the apparatus and then

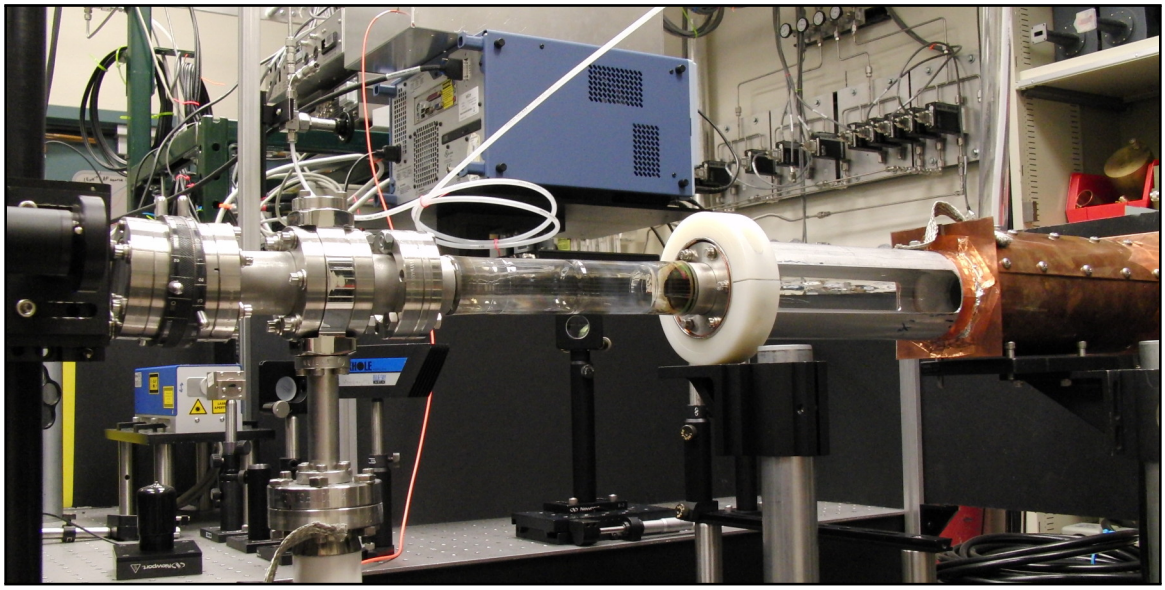

Figure 1.3: Photograph of the discharge apparatus.

sealing it from the pump by all three pump paths. The leak rate was found to be 2.0×10^{-3} sccm. Given a constant flow rate of 25.0 sccm, the fractional impurity can be conservatively estimated to be 80 ppm.

The assembled discharge apparatus can be seen in figure 1.3. The RPND apparatus was supported two 1.5 in mounting posts with angle brackets. The mounting posts attached to a 4 ft by 2.5 ft optical breadboard, supported by urethane shock absorbers, and a rigid frame. The roughing pump was attached to the apparatus with flanged bellows in order to reduce mechanical vibrations.

All electrical measurements were made with a LeCroy 6100A WaveRunner oscilloscope which had a bandwidth of 1.0 GHz. Electrical connections to the oscilloscope were made with RG 50/U coaxial cable and standard BNC connectors. All connections were terminated at 50 Ω unless otherwise noted. The voltage of

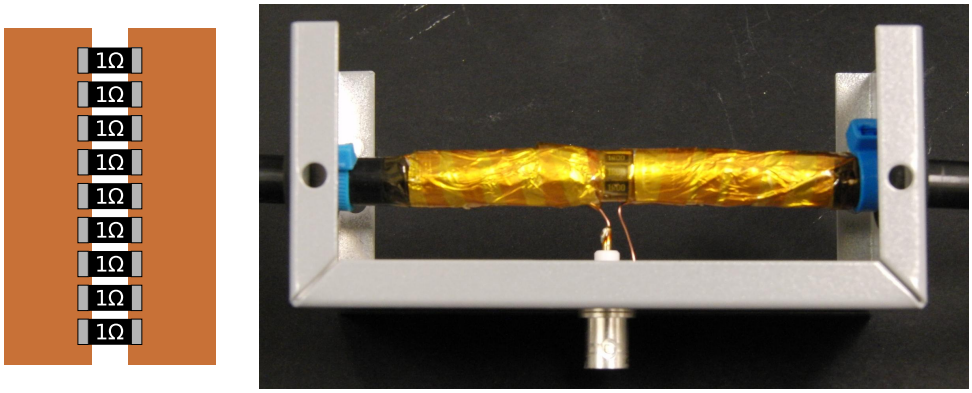

Figure 1.4: Sketch of the unassembled back-current shunt, and a photograph of it assembled around the transmission line.

the pulses was monitored from a 1 : 1000 divider built into the power supply. The current was measured from a current shunt which crossed a small electrical break in the outer conductor of the transmission line. The shunt was built into the transmission line as close as possible to the power supply, about 3 cm from the output connector.

The current shunt was composed of nine, low inductance, 1.0Ω resistors connected in parallel. As illustrated in figure 1.4 the resistors were soldered to two strips of copper foil. This assembly was then wrapped around the electrical break in the transmission line, bridging it. Two short lengths of No. 18 copper wire were soldered to each side of the shunt assembly. These were then attached to a BNC bulkhead connector, fitted to a metal project box. The voltage across the resistors was used to measure the current traveling through the outer conductor of the transmission line. The copper foil was then secured to the outer conductor with several wraps of aluminum foil, followed by a layer of polyimide tape.

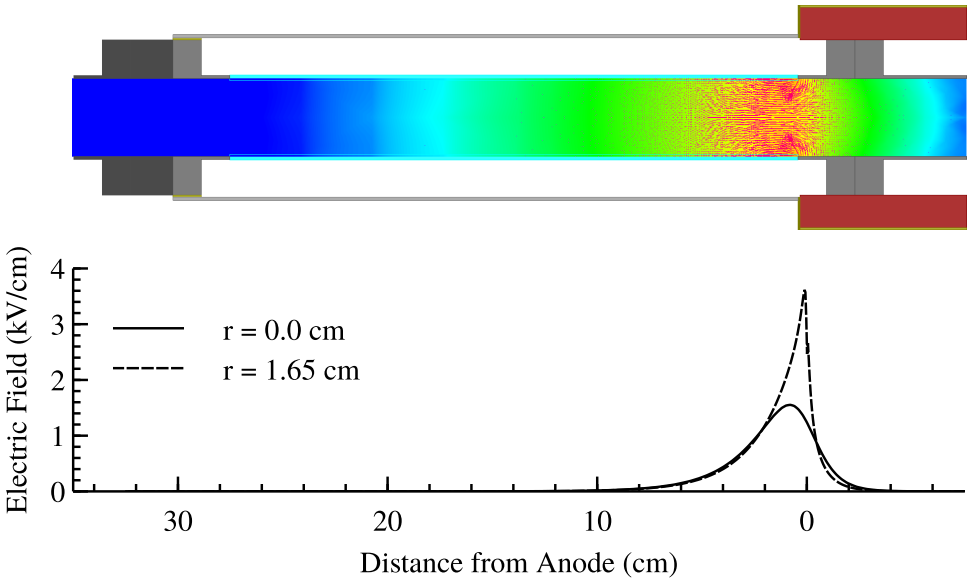

Figure 1.5: Heat map and vector plot of the electric field in the RPND discharge apparatus.

Data were retrieved from the oscilloscope with a desktop computer via the GPIB interface. Instrument control, data acquisition, and data storage were all managed by a LabView program. Analog input and output was handled with the auxiliary input and output ports of a SRS SR850 DSP lock-in amplifier.

1.2 Field Calculations

The electric field characteristics of the discharge apparatus were analyzed using Ansoft Maxwell 9, a two-dimensional, electrostatic solver. At the top of figure 1.5 is a logarithmic heat map of the electric field magnitudes within the device. Overlaid are the electric field vectors in magenta. Below this is a plot of the

electric field on a linear scale, across the central axis of the apparatus and along the outer edge, adjacent to the glass tube. It is apparent that the field strength is the strongest at the triple point which occurs near the glass-metal seal. Also noticeable is the fast fall off of the electric field with distance from the anode. The presence of the external ground shield produces an electric field contour vastly different from that of two parallel plates. This is also reflected in the electric field vectors. Specifically, the many locations possess fields with strong radial components, especially those near the anode.

These characteristics should result in a discharge that is somewhat different than the one-dimensional description of a streamer in chapter **??**. First, assume that the electrons are distributed uniformly throughout the discharge tube, prior to the pulse. As a pulse is applied, ionization would preferentially take place near the anode. As the electrons would be drawn toward the anode, and leave behind some amount of positive space charge. However, as the positive space charge builds up, it would begin to act as a virtual anode, increasing the electric field further from the physical anode. The virtual anode would then begin to draw its own electron current, predominantly from around the edges, near the wall. In this manner, the discharge would propagate away from the anode, leaving a quasineutral ionized gas in the center of the discharge tube and a positive space charge region along the wall.

1.3 Operating Procedures

One of two operating procedures for the RPND was used depending on how recently the discharge had last been turned on. If it had been greater than one hour, a full startup procedure was used. Otherwise, an abbreviated process was used.

In the case that the discharge had not been operated for over an hour, the roughing pump was turned on and the primary pump path valve was opened as was the first shutoff valve upstream of the discharge chamber, seen in figure 1.2. The system was then allowed to pump down to its base pressure. Afterward the second upstream shutoff valve was opened and the system was again allowed to reach base pressure. At this point the helium flow was turned on and set to 25.0 sccm. The primary pump path was then closed and the needle valve bypasses were used to adjust the system pressure to 3.0 Torr.

Next, the delay generator was turned on and the output for triggering the power supply was activated. Then, the FID power supply was turned on. This would produce an easily visible discharge within the discharge tube. The system was allowed to operate at this condition for one hour in order to remove potential contamination on the walls and electrodes. At the end of this period, the voltage waveform was checked to ensure that it was consistent with previous experiments. Once this was confirmed, the pressure was adjusted to the desired operating condition.

The discharge was shutdown by first shutting off the power supply, followed by the delay generator. Then, the helium flow was shut off, and the primary pump

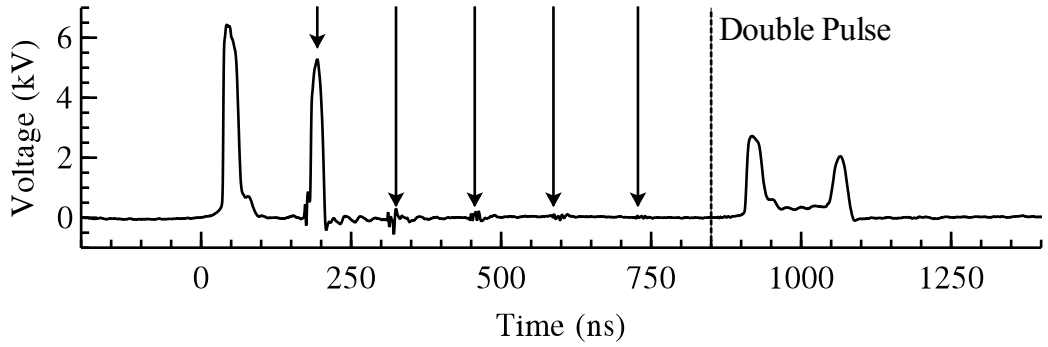

Figure 1.6: Typical voltage waveform of the RPND. Arrows indicate reflections back to the power supply. The dotted line delineates the time at which the power supply begins to exhibit double pulsing.

path was opened. The system was allowed to come to base pressure before the two upstream shutoff valves were closed, after which the primary pump path was closed. The roughing pump was then shut off.

In the cases that the discharge had been operated within the last hour, it was possible to use an abbreviated startup procedure. This process was fundamentally the same as the previous one, however the discharge only required five minutes to reach a steady state. This was verified with multiple measurements of the current and voltage characteristics as well as the discharge emissions. At times prior to this five minute equilibration period, the reflected pulse energy was noticeably higher, and the delay between the trigger pulse and the output pulse was variable.

1.4 Electrical Characteristics

The typical voltage waveform, as seen in figure 1.6, exhibited a number of fea-

tures. It begins with an incident pulse at $t = 0.0$. 138 ns later, it is followed by the pulse that has been reflected from the anode. The reflected pulse is somewhat smaller, proportional to the energy deposited in the discharge. Additional reflections are visible at integer multiples of 138 ns. These subsequent reflections are much smaller than the initial one, suggesting that much of the remaining pulse energy was dissipated after the first reflection reached the anode. Curiously, a second pulse appears at 800 ns. This is believed to be a peculiarity of the power supply. For the most part, analysis of the RPND will focus on the times which precede 280 ns (the incident pulse and first reflected pulse).

The properties of the RPND were examined at: 0.3, 0.5, 1.0, 2.0, 3.0, 4.0, 8.0, and 16.0 Torr. The appearance of the discharge varied with the pressure in a continuous fashion, however it was apparent that there were three regimes of operation. At the low pressures, 0.3 and 0.5, it was difficult to initiate the discharge. Often, it would be necessary to increase the pressure to initiate the discharge, and then reduce the pressure to the desired conditions. The discharge appeared dim and relatively constricted about the central axis of the discharge tube, with a radial extent of approximately 1 cm. Accompanying these pressures was a large degree of electronic noise. This manifested primarily in the current waveforms, as seen in figure 1.7, as well as a number of equipment malfunctions.

As the pressure was increased (from 1.0-4.0 Torr), the electrical noise began to subside. The current waveforms in showed significant reductions in the ringing that was particularly prominent at lower pressures. In addition, the visual extent of the discharge increased substantially, to the point where it could be

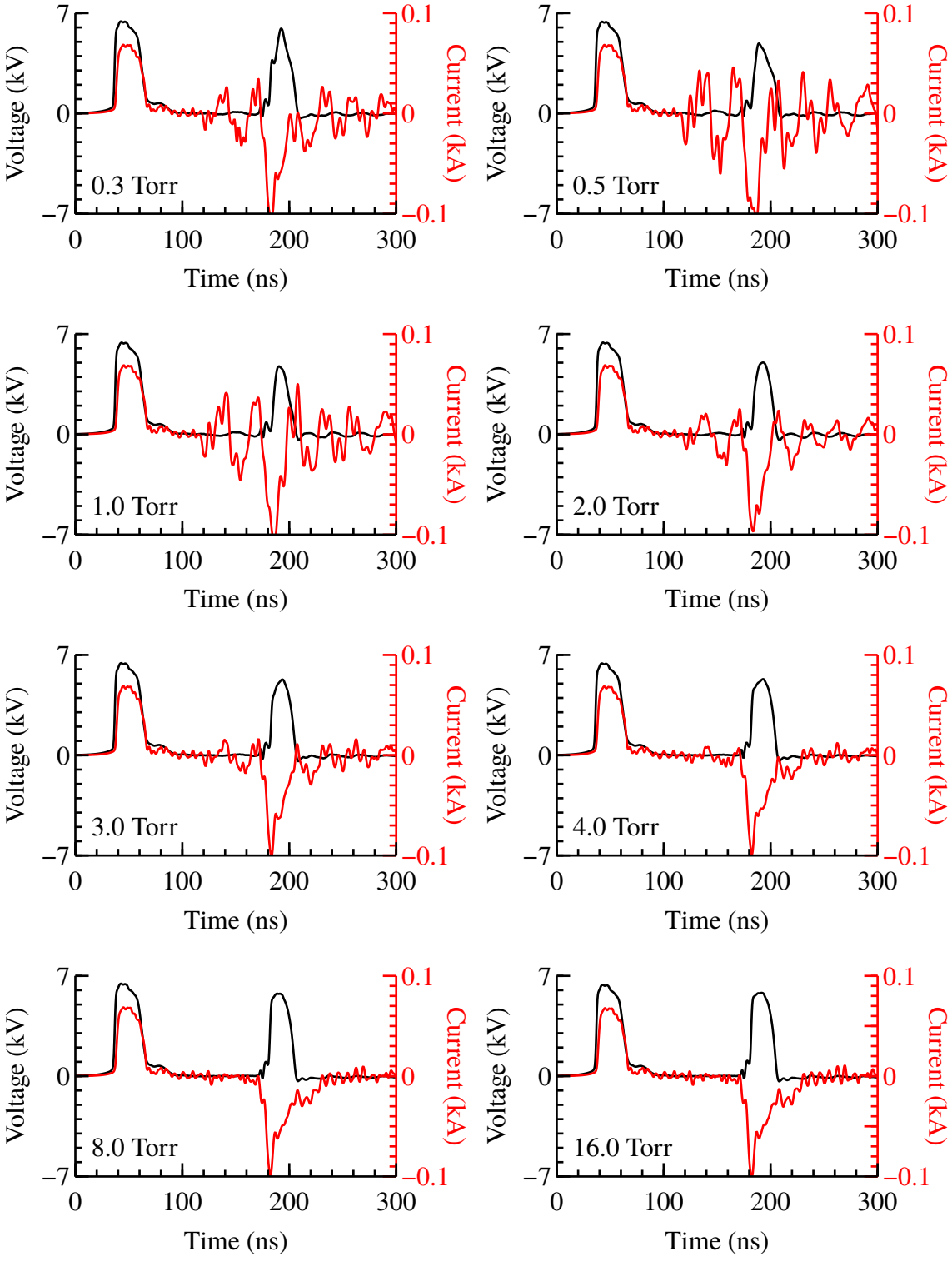

Figure 1.7: High resolution views of the voltage and current waveforms for the first incident and reflected pulse, at each of the operating pressures.

considered volume-filling. The discharge also increased its axial extent as well, eventually reaching well past its intended limit at the cathode. This occurred despite attempts to isolate the downstream pump sections from the discharge. It is possible to attribute this to the relatively large surface area of the anode in comparison to the cathode.

The discharge receded back to the intended cathode structure at the higher operating pressures, 8.0 and 16.0 Torr. This was accompanied by a decrease in the apparent brightness of the discharge to levels similar to that of the low pressure conditions. In contrast, the discharge appeared to remain volume-filling. While discharge initiation was difficult at the higher pressures, it was not accompanied by the electrical noise observed at lower pressures.

1.5 Energy Coupling

The product of the voltage and current waveforms, as seen in figure 1.7, gives the power deposited in the discharge as a function of time. Subsequently, the power integrated over time gives the total energy deposited in the discharge. However, this approach is somewhat complicated by several features of the RPND. As previously mentioned, the pulses produced by the power supply are not completely absorbed by the discharge. Therefore, the integration must be carried out over both the incident and the reflected pulse. Additionally, there is the concern that the oscillations in the current measurements could introduce fluctuations in the calculated energy deposition. However, the small voltage signal limits the error

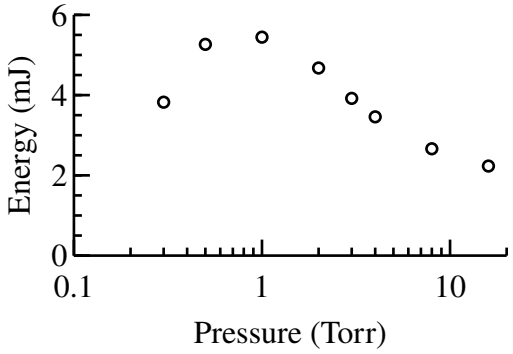

Figure 1.8: Plot of the energy coupled into the discharge with the first pulse as a function of pressure.

introduced by these fluctuations to less than 1%.

Figure 1.8 gives the total energy deposited for the first pulse at each of the operating conditions. The energy coupled to the discharge peaks at an energy of 5.5 mJ at a pressure of 1.0 Torr, after which it slowly decreases. This peak in the coupled energy is coincident with the peak brightness of the discharge. Together, these suggest that the density of excited states will be optimized at intermediate pressures.

Though there appear to be no direct comparisons available in the literature, several papers report on energy coupling for similar systems. Macheret, Schneider, and Murray studied a parallel plate RPND in air, at 1-10 Torr and reported a total energy deposition of 0.30-0.36 mJ, increasing with pressure [2]. Nishihara et al. recorded values of 1-2 mJ in a nitrogen RPND [3]. Pancheshnyi et al., in the study of an air-propane mixture at 750 Torr, found that each pulse deposited about 1.9 mJ of energy. Overall, the measured values for the deposited energy

appear to be in comparable with those previously measured.

From an applications standpoint, the potential existence of a condition which optimizes the production of excited states is an interesting one. This behavior is also compelling from a physical standpoint as it suggests a phase change in the competition of two or more processes. Though this kind of competition is reminiscent of Paschen's law, the duration of the pulse is too short for appreciable ion drift to occur (an estimated maximum of 3 mm), therefore secondary electron emission is not important. These observations provide further impetus for a close examination of the RPND properties, particularly the excited state dynamics.

Bibliography

[1] L M Vasilyak, S V Kostyuchenko, N N Kudryavtsev, and I V Filyugin. Fast ionisation waves under electrical breakdown conditions. *Physics-Uspekhi*, 37(3):247–268, March 1994.

[2] S. O. Macheret, M. N. Shneider, and R. C. Murray. Ionization in strong electric fields and dynamics of nanosecond-pulse plasmas. *Physics of Plasmas*, 13(2):023502, 2006.

[3] Munetake Nishihara, J. William Rich, Walter R Lempert, Igor V. Adamovich, and Sivaram Gogineni. Low-temperature M=3 flow deceleration by Lorentz force. *Physics of Fluids*, 18(8):086101, 2006.